Heliyon 9 (2023) e16222

Contents lists available at ScienceDirect

Heliyon

journal homepage: www.cell.com/heliyon

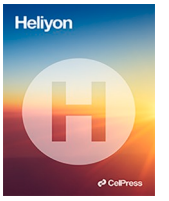

Research article

Synthesis, characterization, antibacterial activity of thiosemicarbazones derivatives and their computational approaches: Quantum calculation, molecular docking, molecular dynamic, ADMET, QSAR

Mahbub Alam [a], Mohammed Nurul Abser [a,*], Ajoy Kumer [b,**], Md Mosharef Hossain Bhuiyan [c], Parul Akter [d], Md Emdad Hossain [e], Unesco Chakma [b,f]

[a] *Inorganic Research Laboratory, Department of Chemistry, Jahangirnagar University, Savar, Dhaka, 1342, Bangladesh*
[b] *Laboratory of Computational Research for Drug Design and Material Science, Department of Chemistry, European University of Bangladesh, Dhaka, 1216, Bangladesh*
[c] *Department of Chemistry, University of Chittagong, Chittagong, 4331, Bangladesh*
[d] *Department of Chemistry, Mirzapur Cadet College, Mirzapur, Tangail, 1942, Bangladesh*
[e] *Wazed Miah Science Research Centre, Jahangirnagar University, Savar, Dhaka, 134, Bangladesh*
[f] *School of Electronic Science and Engineering, Southeast University, Nanjing, PR China*

ARTICLE INFO

Keywords:
Aldehyde
Thiosemicarbazide
Dicyclohexylcarbadiimide
Dimethylaminopyridine
Thiosemicarbazones
Antibacterial activity

ABSTRACT

The thiosemicarbazones and their derivatives have been recognized as antimicrobial agents against human pathogenic bacteria and fungi. Regarding these prospective, this study was designed to address the new antimicrobial agents from thiosemicarbazones and their derivatives. These derivatives were synthesized by multi-step synthesis methods, such as alkylation, acidification, esterification, and formed the 4-(4′-alkoxybenzoyloxy) thiosemicarbazones and its derivatives (THS1, THS2, THS3, THS4, and THS5). Afterward the synthesis, compounds were characterized by ^{1}H NMR, FTIR spectra, and melting point. Later, the computational tools were applied to evaluate the drug likeness properties, bioavailability score, Lipinski rule, absorption, distribution, metabolism, excretion, and toxicity (ADMET). Secondly, the quantum calculations, for instance HOMO, LUMO and chemical descriptors, were calculated by the density functional theory (DFT). Finally, the molecular docking was performed against seven human pathogenic bacteria, black fungus (Rhizomucor mieh, Mucor lusitanicus, Mycolicibacterium smegmatis) and white fungus strains (Candida Auris, Aspergillus luchuensis, Candida albicans). To check and validate of molecular docking procedure and stability of docked complex for ligand and protein, the molecular dynamic was performed of docked complex. From the docking score with calculating the binding affinity, these derivatives could show a higher affinity than standard drug against all pathogens. From the computational details, it could be decided to do *in-vitro* test as antimicrobial activity against Staphylococcus aurious, Staphylococcus homonis, *Salmonella typhi*, and Shigella flexneria. The obtained result of antibacterial activity compared to standard drugs, and it was found that the synthesized compounds were almost same value of standard drug.

* Corresponding author.
** Corresponding author.
E-mail addresses: abserju@yahoo.com (M.N. Abser), kumarajoy.cu@gmail.com (A. Kumer).

https://doi.org/10.1016/j.heliyon.2023.e16222
Received 2 February 2023; Received in revised form 4 May 2023; Accepted 10 May 2023
Available online 24 May 2023

Finally, it could be said from the *in-vitro* and *in-silico* study that the thiosemicarbazones derivatives are good antimicrobial agents.

1. Introduction

The thiosemicarbazone is organometallic aromatic compounds which are formed between chelating ligands with transition metal ions by bonding through the sulfur and/or hydrazinic nitrogen atoms [1]. As a result, these organometallic aromatic compounds demonstrate sky-scraping affinity for sulfur and nitrogen containing biomolecules, such as amino acids (cysteines and methionines), peptides (glutathione) and proteins (metallothionein) [2]. In addition, the thiosemicarbazone-appended aromatic compounds have been being paid noteworthy attention in the vicinity of medicine, drug design and biochemistry due to their effective biological effects and outstanding pharmacological properties, for example antimicrobial agent, antibacterial, antifungal, antimalarial, antiviral, even dengue virus [3]. Besides, metal thiosemicarbazone complexes are rising as new class of investigational anticancer chemotherapeutic agents which show inhibitory activities against various type of cancer because the nitrogen and sulfur atoms act donor ligands particularly for transition metal ions to form internal hydrogen and hydrophilic bonds with protein of cancer. As a result, they were already used as antiparasitic [4], potential *anti*-trypanosomal agents [5], antitumor activities [6], nuclear medicine [7] and anticancer activities [8]. In addition, last one decade, they had also estimated the parasiticidal activity against *Plasmodium falciparum*, *Plasmodium berghei*, *Trypanosoma cruzi*, *Trypanosoma bruceirhodesiense* and *Toxoplasma gondii* [9]. Due to having vast applications as bioactive molecules in medicinal chemistry, this study has been designed and investigated for synthesis and antimicrobial activity with their computational and *in silico* study.

In general, the synthesis of thiosemicarbazone consists of a condensation reaction between an aldehyde and a thiosemicarbazide by the multi-step synthesis methods where the aldehydes are modified by introducing an additional ester linkage group containing long alkyloxy chain before condensation reaction [10]. The FTIR, ^{1}H NMR, and melting point were used for characterization and conversion of reaction for synthesized compounds after purification. Before, the synthetic study, the computational tools have performed to design the molecules of thiosemicarbazones.

In recent times, computational chemistry has taken much awareness due to numerous benefits, such as its low cost, sustainable environment, and no waste chemicals even low employment cost. As a result, the computational tools are the first choice for designing a drug with *in silico* study [11,12], where the Density Functional Theory (DFT) is one of the most accurate method to determine the quantum parameters or molecular optimization of atom or molecules [13–17]. In addition, it has been executed for calculating the chemical descriptors. Then, the HOMO, LUMO, energy gap, hydrophilic and hydrophobic nature has been predicted for thiosemicarbazones and its derivatives. As these derivatives have the potential activity against antifungal or infection diseases, they have docked against the human pathogenic bacteria strain, black fungus, and white fungus strain. Moreover, the molecular docking study conveys the binding affinity, binding site, and residue of protein of pathogens with the mechanism of attachment [18–23]. Finally, the docking score can be able to predict the potential of defined protein and the docking procedure is further justified by molecular dynamic study. The Root Mean Square Deviation (RMSD) and Root Mean Square Fluctuation (RMSF) have been calculated after performing the molecular dynamic simulation that confirms information about stability and validation of docking procedure for the docked complex of ligand and protein throughout the water or biological system. Afterward of the computational and *in silico* investigation, the antimicrobial activity has been performed to compare with the docking study, and experimental result.

2. Methodology and materials

2.1. Computational details

2.1.1. Optimization of ligand and determination of chemical descriptors

DMol3 code of material studio 08 [24], is one of the most used software package for molecular optimization. Using this software, the B3LYP functional and DND basis set was executed due to the presence of the electronegative atom, like oxygen, though DFT functional. Regarding the molecular optimization by DFT method, the structural geometry and electronic structure were studied for confirming the molecular optimization in minimum energy. After optimization, the molecules were saved for further analysis. The εLUMO, εHOMO and energy gap (ΔE) gap, ionization potential (I), electron affinity (A), chemical potential (μ), electronegativity (χ), hardness (η), softness (s) and electrophilicity (ω) were calculated and presented in Table 1 using equations (1)–(8).

$$E_{gap} = (E_{LUMO} - E_{HOMO}) \ldots\ldots\ldots \quad (1)$$

$$I = -E_{HOMO} \ldots\ldots\ldots\ldots \quad (2)$$

$$A = -E_{LUMO} \ldots\ldots\ldots\ldots \quad (3)$$

$$(\chi) = \frac{I + A}{2} \ldots\ldots\ldots\ldots\ldots\ldots \quad (4)$$

$$(\omega) = \frac{\mu^2}{2\eta} \ldots\ldots\ldots\ldots\ldots\ldots \quad (5)$$

$$(\chi) = -\frac{I + A}{2} \ldots\ldots\ldots\ldots\ldots\ldots\ldots \quad (6)$$

$$(\eta) = \frac{I - A}{2} \ldots\ldots\ldots\ldots\ldots \quad (7)$$

$$(S) = \frac{1}{\eta} \ldots\ldots\ldots\ldots\ldots\ldots\ldots \quad (8)$$

2.1.2. Determination Lipinski rule and drug likeness properties

Swiss ADME online free website (http://www.swissadme.ch/) was used to assess the Lipinski rule of five and pharmacokinetics [25].

2.1.3. ADMET calculation

The ADMET facial appearances were demonstrated using the online database amdetSar (http://lmmd.ecust.edu.cn/admetsar2), that is the most ideal database for calculating the AMDET features [26–28].

2.1.4. Preparation of protein and procedure for molecular docking

For molecular docking, the preliminary three-dimensional (3D) structure of protein is required which was collected from Protein Data Bank (PDB) (https://www.rcsb.org/). Three proteins of triple-negative breast cancer (PDB ID: 4PV5), cervical cancer (PDB ID: 1A7T) & colon carcinoma (PDB ID: 1J26) were downloaded from the PDB. The raw proteins from the PDB were taken in the PyMOL program version PyMOL V2.3 (https://pymol.org/2/) [29] for preparation and optimization after removing water molecules and unusual ligands or heteroatoms to make a new fresh protein. Finally, it was exported as PDB file. Secondly, in this case of performing the auto dock vina, the PyRx program [30] was applied for molecular docking while the grid box parameters was used as center X = 12.4697, Y = 15.9818, Z = 16.0634, and Dimension (Å) X = 35.144, Y = 37.645 Å, and Z = 36.966 Å. Next, the docked compounds were then uploaded to Discovery Studio version 2017 for overall results and viewing after molecular docking [31].

2.1.5. Molecular dynamic

To explore the dynamic interactions of molecules in materials and biological sciences, MD simulation is an effective method [32, 33]. In order to execute MD simulations, NAMD methodology was employed on a desktop computer in batch mode or dynamically with a live view computer. For holo-form (drug-protein) docking, AMBER14 force field simulation has been used to ensure the perfect match and stability of the protein-ligand complexes up to 500 ns (39). At 298 K, the whole system was equilibrated accurately adding 0.9% NaCl in the medium of a water solvent in presence of liquid system with NVT ensemble having the simulation box size as boundary 1.5 and X = 5, Y = 5 and Z = 5 which is standard for these proteins for solvation, as well as, its vector coordinate of box is at −25.06, 18.79 and −7.06, respectively. VMD evaluated the performance of this result using RMSD and RMSF. During the simulation, a cubic cell box was replicated inside 20 Å on every corner of the operation and periodic area circumstances.

2.2. Materials and synthesis

2.2.1. Chemicals

Thiosemicarbazide, alkyl bromide, cyclohexanone, methanol, ethanol, 1-butanol, dimethyl aminopyridine (DMAP), dichloromethane (DCM), acetone, sodium hydroxide, and potassium carbonate were used. Methanol and ethanol were distilled over anhydrous calcium oxide. Dichloromethane was also distilled, and acetone was dried over molecular sieves. All other chemicals used were laboratory grade. Pre-coated silica gel aluminum sheet (silica gel 60, F-254, 0.25 mm) from E-Merck was used for analytical thin-layer chromatography (TLC).

2.2.2. Techniques

1H NMR spectra were recorded on a spectrophotometer (Bruker Avence III HD spectrometer-400 MHz) from Chloroform-D solution while TMS as internal standard at Wazed Miah Science Research Centre (WMSRC), JU. FTIR spectra were recorded on Shimadzu spectrophotometer Prestige 21 with KBr pellets in the range of 4000–400 cm^{-1}. Concentration was done by Rotavapor (BÜCHI; R-114), progress of the reaction and purity of the products were monitored by TLC. The melting point was recorded by Polarizing Microscope fitted with a hot and cold stage, and was used to identify the mesophases. Olympus CX Polarizing Microscope fitted with INSTEC Hot and Cold stage HCS 402 and computer-operated controller INSTEC MK 1000 was used. Antibacterial tests were performed at the department of biochemistry in the University of Chittagong, Chittagong, Bangladesh.

2.3. Synthesis and purification of thiosemicarbazones

The thiosemicarbazide compound was dissolved in 10 ml of 1-butanol in a hot state, and ester linkage aldehyde was also dissolved

in 10 ml of 1-butanol. Then the dissolved thiosemicarbazide was added from the beaker with a dropper in the ester linkage solution. A clear solution was formed, a drop of glacial acetic acid was used in the reaction mixture as a catalyst, and the reaction mixture was refluxed for 2/3 h. So, thiosemicarbazone formation was checked by TLC using solvent DCM and cyclohexane (1:1). The mixture was filtered by using a small Buckner funnel. The product was recrystallized by using solvent DCM and methanol. The formations of thiosemicarbazones were characterized by FTIR, 1H NMR, and melting point. Five derivatives of THS (THS1, THS2, THS3, THS4 and THS5) were synthesized by using following reaction scheme in Fig. 1.

2.4. Characterization

The compoundTHS1 showed resonance signals with different δ (chemical shift) values. The signals in the region at 7.00 ppm (2H, d) and 8.16 ppm (2H, d) are for the protons of H4 and H5, the coupling constant is at 8.8 Hz, probably these are the protons of the ring B. Again, the signal at 7.73 ppm (d, 2H) and 7.43 ppm (d, 2H) is for the protons of H6 and H7, the coupling constant is at 8.80 Hz, almost certainly these are the protons of the ring A. The proton of –C═NH gives a signal at 7.93(1H, s), the proton of $–NH_2$ and –NH- gives signals at 6.48 ppm (br.) and 9.91 ppm (br.), respectively. The aliphatic protons numbered as 6, 7, 8, 9, 10, 11, 12 give the signal at 4.06 ppm (triplet), at 1.86 ppm (multiplet), at 1.48 ppm (multiplet), at 1.30 ppm (multiplet) and at 0.86 ppm (triplet), respectively.

The compoundTHS1 showed absorption band at υH-N (str) = 3394.72 (br) are for H– N bond stretching, υH-N-H (str) = 3284.77, 3342.34 (br) are for H– N–H bond stretching, υC-H (str) = 3051.39 is for aromatic C–H bond stretching, υC-H (str) = 2916.37 and 2848.86 cm^{-1} are for aliphatic C–H bond stretching, υC═O (str) = 1710.86 cm^{-1} is due to C═O bond stretching of ester, υC═C (str) = 1600.92 cm^{-1} for aromatic C═C bond stretching, υC═N (str) = 1510.26 cm^{-1} for aromatic C═N bond stretching, υC-H (ben) = 1417.68 cm^{-1} is due to C–H bending in $–CH_2$-, υC-H (bend) = 1315.45 cm^{-1} is due to C–H bending in $–CH_3$, and υC-O (str) = 1232.51–1008.77 cm^{-1} are due to C–O bond stretching.

The chemical shift values & FTIR absorption band(THS2, THS3, THS4 and THS5)of other compounds are found to be almost the same which evidence confirms their chemical conversion and their chemical structure.

4-(4′-decyloxybenzoyloxy)thiosemicarbazone(THS1)Yield: 68%, mp: 189 °C

^{1}H NMR ($CDCl_3$) (400 MHz) δ, ppm:[8.16, d, 2H(5), J = 8.8], [7.73, d, 2H(6), J = 8.8], [7.300, d, 2H(7)], [7.00, d, 2H(4), J = 8.8], [7.93, s, 1H], [9.91, br.1H], [6.48, br. 2H], [4.06, t, 2H], [0.88–1.86 for aliphatic protons 8–12].

IR (KBr, υ$^-$, cm^{-1}): 3394.72 cm^{-1} (-N-H stretching), 3284.77, 3242.34 cm^{-1} (H–N–H stretching), 3070.68 cm^{-1} (aromatic C–H), 2916.37, 2828.86 cm^{-1} (aliphatic C–H), 1710.86 cm^{-1} (C═O group), 1510.26 cm^{-1} (aromatic C═C), 1600.82 cm^{-1} (C═N bond), 802.14 cm^{-1} (C═S bond).

4-(4′-dodecyloxybenzoyloxy)thiosemicarbazone(THS2): Yield: 76%, mp: 190 °C

^{1}H NMR ($CDCl_3$) (400 MHz) δ, ppm:[8.16, d, 2H(5), J = 8.4], [7.73, d, 2H(6), J = 8.4], [7.30, d, 2H(7)], [7.01, d, 2H(4), J = 8.8], [7.89, s, 1H], [9.65, br.1H], [6.41, br. 2H], [4.06, t, 2H], [0.89–1.86 for aliphatic protons 8–12.

IR (KBr, υ$^-$, cm^{-1}): 3425.58 cm^{-1} (-N-H stretching), 3398.57, 3273.20 cm^{-1} (H–N–H stretching), 3070.68 cm^{-1} (aromatic C–H), 2920.23, 2828.86 cm^{-1} (aliphatic C–H), 1722.43 cm^{-1} (C═O group), 1508.33 cm^{-1} (aromatic C═C), 1598.99 cm^{-1} (C═N bond), 806.14 cm^{-1} (C═S bond).

4-(4′-tetradecyloxybenzoyloxy)thiosemicarbazone(THS3):Yield: 70%, mp: 213 °C

^{1}H NMR ($CDCl_3$) (400 MHz) δ, ppm:[8.16, d, 2H(5), J = 8.8], [7.74, d, 2H(6), J = 8.4], [7.31, d, 2H(7)], [7.00, d, 2H(4), J = 8.4], [7.86, s, 1H], [9.38, br.1H], [6.36, br. 2H], [4.067, t, 2H], [0.88–1.86 for aliphatic protons 8–12.

IR (KBr, υ$^-$, cm^{-1}): 3404.36 cm^{-1} (-N-H stretching), 3284.77, 3250.05 cm^{-1} (H–N–H stretching), 3070.68 cm^{-1} (aromatic C–H), 2916.37, 2828.86 cm^{-1} (aliphatic C–H), 1735.93 cm^{-1} (C═O group), 1506.26 cm^{-1} (aromatic C═C), 1602.45 cm^{-1} (C═N bond), 803.35 cm^{-1} (C═S bond).

4-(4′-hexadecyloxybenzoyloxy)thiosemicarbazone(THS4):Yield: 75%, mp: 201 °C

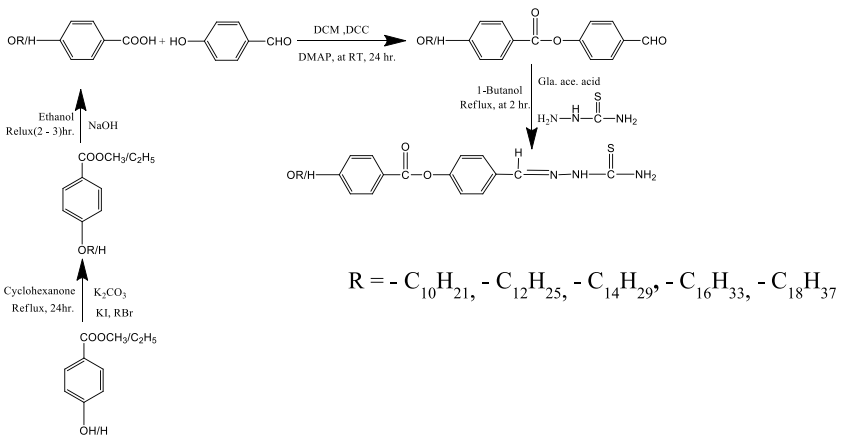

Fig. 1. Reaction Scheme for synthesis.

^{1}H NMR ($CDCl_3$) (400 MHz) δ, ppm:[8.16, d, 2H(5), J = 7.6], [7.73, d, 2H(6), J = 7.2], [7.30, d, 2H(7), J = 9.2], [7.00, d, 2H(4), J = 8.00], [7.86, s, 1H], [9.93, br.1H], [6.37, br. 2H], [4.07, t, 2H], 0.90–1.84 for aliphatic protons 8–12.

IR (KBr, υ$^-$, cm^{-1}): 3423.65 cm^{-1} (-N-H stretching), 3321.42, 3250.05 cm^{-1} (H–N–H stretching), 3070.68 cm^{-1} (aromatic C–H), 2918.30, 2828.86 cm^{-1} (aliphatic C–H), 1726.29 cm^{-1} (C═O group), 1510.26 cm^{-1} (aromatic C═C), 1604.77 cm^{-1} (C═N bond), 801.55 cm^{-1} (C═S bond).

4-(4′-octadecyloxybenzoyloxy) thiosemicarbazone (THS5): Yield: 69% mp: 204 °C

^{1}H NMR ($CDCl_3$) (400 MHz) δ, ppm:[8.16, d, 2H(5), J = 6.8], [7.74, d, 2H(6), J = 6.40], [7.300, d, 2H(7)], [7.00, d, 2H(4), J = 6.8], [7.83,s, 1H], [9.21,br.1H], [6.33, br. 2H], [4.07,t, 2H], 0.90–1.84 for aliphatic protons 8–12.

IR (KBr, υ$^-$, cm^{-1}): 3415.93 cm^{-1} (-N-H stretching), 3284.77, 3265.49 cm^{-1} (H–N–H stretching), 3070.68 cm^{-1} (aromatic C–H), 2954.95, 2828.86 cm^{-1} (aliphatic C–H), 1734.01 cm^{-1} (C═O group), 1510.28 cm^{-1} (aromatic C═C), 1600.92 cm^{-1} (C═N bond), 804.64 cm^{-1} (C═S bond).

2.5. Biological activity

2.5.1. Preparation of solution

The certain concentration of the solution of thiosemicarbazones was prepared, so that there were no impurities. For various concentrated solutions were used for the determination of inhibition zones.

2.5.2. Antibacterial activity

To primary screening of antibacterial activity of synthesized THS, the four human bacterial pathogens, for instance *Staphylococcus aureus, Staphylococcus hominis, Salmonella Typhi, Shigella flexneria* were taken. The disc diffusion method was carried on taking 100 μg (dw)/disc. After completing the working progress for the good diffusion method, the Petri dish was kept in an incubator at 36–37 °C for overnight for the growth of bacteria strain. Then, the zone of inhibition was measured on an mm scale with thoughtfulness 1.0 mm errors. This working progress was done in triple times, and the average magnitudes were listed in Table S8. It is noted that DCM was used as a solvent to prepare THS solutions. As a result, DCM was considered as controlled.

3. Result and discussion

3.1. Optimized structure

The opening obsession that locates out in computational chemistry is to categorize the stable configuration of any molecular structure. These all molecules are optimized through the DFT functional with taking suitable configuration, and it has been observed that their symmetry is extremely similar. The optimized structure has been presented in Fig. 2. According to optimized structure, the obtained bond distance of C–C is at 1.53639 A° where the C–C bond distance is at 1.54 Å in view of experimental value. Secondly, the C–O bond is found at 1.50899 Å while the experimental value is 1.54 Å shown in Table S9. So, the optimized structure after DFT optimization is accurate.

3.2. HOMO, LUMO and chemical reactivity descriptors

The chemical identifiers have sole importance for every chemical molecule or chemical active compounds. It is a well-established concept for accounting for energy gap indicates the stronger their chemical reactivity, which is allowing them to engage in chemical processes more effectively reactions. In addition, as the value of hardness rises, the object's susceptibility to degrade diminishes and its

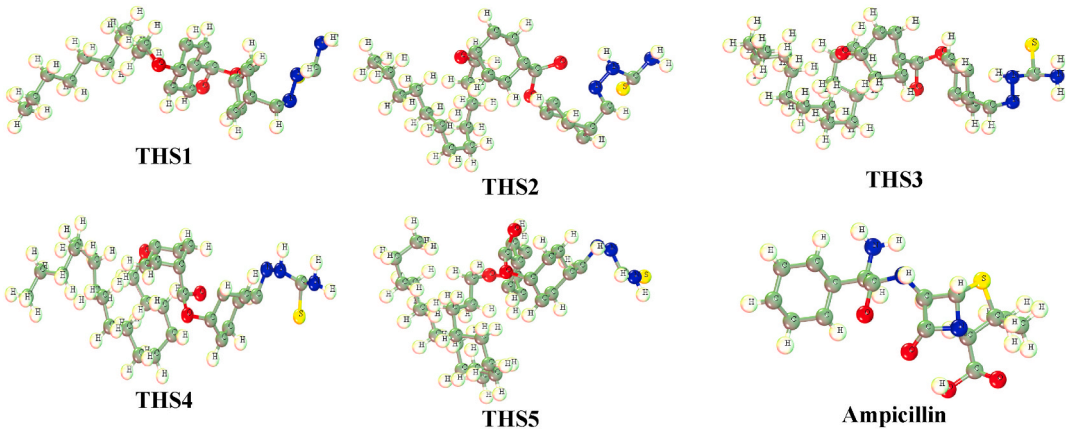

Fig. 2. Optimized structure of molecules.

Table 1
Frontier molecular orbitals and reactivity descriptor analysis.

	εLUMO, eV	εHOMO, eV	εHOMO εLUMO gap, eV	Ionization potential (I), eV	Electron affinity (A), eV	Chemical potential (μ), eV	Hardness (η), eV	Electrons activity (χ), eV	Electrophilicity (ω), eV	Softness (S), V
THS1	−1.453	−8.153	6.700	8.153	1.453	−4.803	3.350	4.803	3.443	0.299
THS2	−3.17	−8.349	5.179	8.349	3.170	−5.760	2.590	5.760	6.405	0.386
THS3	−2.625	−8.702	6.077	8.702	2.625	−5.664	3.039	5.664	5.278	0.329
THS4	−3.290	−8.049	4.759	8.049	3.290	−5.670	2.380	5.670	6.754	0.420
THS5	−3.539	−7.997	4.458	7.997	3.539	−5.768	2.229	5.768	7.463	0.449
Ampicillin	−2.740	−9.551	6.811	9.551	2.740	−6.146	3.406	6.146	5.545	0.294
Starting	−2.262	−9.797	7.535	9.797	2.262	−6.030	3.768	6.030	4.825	0.265

acceptability as an active medication continuously diminishes. On the other hand, the biological activity is closely related to the softness index and handedness which are opposite to each other at quantitative value. From Table 1, it is found that the energy gap for THS1 is at 6.70 eV which is reduced with an increasing alkyl chain of molecules, and it is shifted at 5.100 eV, 6.077 eV, 4.758 eV, and 4.458 eV for THS2, THS3, THS4, and THS5, respectively. In case of starting, the energy gap is at 7.535 eV that was reduced after forming complexes. In addition, these obtained values (energy gap) for THS1, THS2, THS3, THS4, and THS5 are smaller than starting and standard (Ampicillin). Finally, the smallest value of energy gap is obtained for THS5. So, it could be said that all derivatives are chemically more stable than starting material which is derived similar trend from the ionization potential, chemical potential, electron affinity, and electrons activity. When it comes to the bioactivity of a compound, the lower degree of softness is much more effective while the larger value of hardness indicates the highest stability. The softness value of THS5 is the highest (0.449) and the lowest (0.299) for THS1 while the hardness of THS1 is the highest value (3.350) and the lowest value is 2.229 for THS5.

3.3. Frontier molecular orbital: HOMO and LUMO

In the accurate appraisal of the determination of the active site on molecules, the HOMO and LUMO orbitals play a significant role in their electrophilic and hydrophobic attraction with biological micromolecules [34–36]. The HOMO and LUMO orbital geometries have been ascertained utilizing DFT technique. As it can be observed from Fig. 3, LUMO is often present in parts containing oxygen atoms of the benzene ring of the thiosemicarbazone ring while the moron color is the positive node of orbital and yellow color is the negative color. Moreover, it is revealed that the LUMO is observed for the almost same part for THS1, THS2, THS3, THS4 and THS5. The main cause is explained that due to the presence of electron-negative atom (Oxygen) near to the benzene ring, the LUMO portion has obtained at this region. On the other hand, the HOMO has obtained the sulfur and nitrogen atoms containing the part in the thiosemicarbazone ring whereas the light blue color is a positive node of orbital and light orange color indicates the negative node of the orbital. So, electrophilic part of the protein can be attracted by the thiosemicarbazone due to having HOMO part on sulfur and nitrogen atoms.

3.4. Electrostatic potential charge distribution map

In investigations of a wide range of molecular interactions, map of electrostatic potential (MEP) has become a key factor of reactivity measurement or scale for chemical species [37]. The effectiveness of this theoretical approach in investigations and analysis of physical, biological, and associated operations is widely estimated by the active site of orbital [38–40]. When studying to discover bioactive compounds, MEP illustrates the independently methodologies and active site of charge carrying portion of molecules which

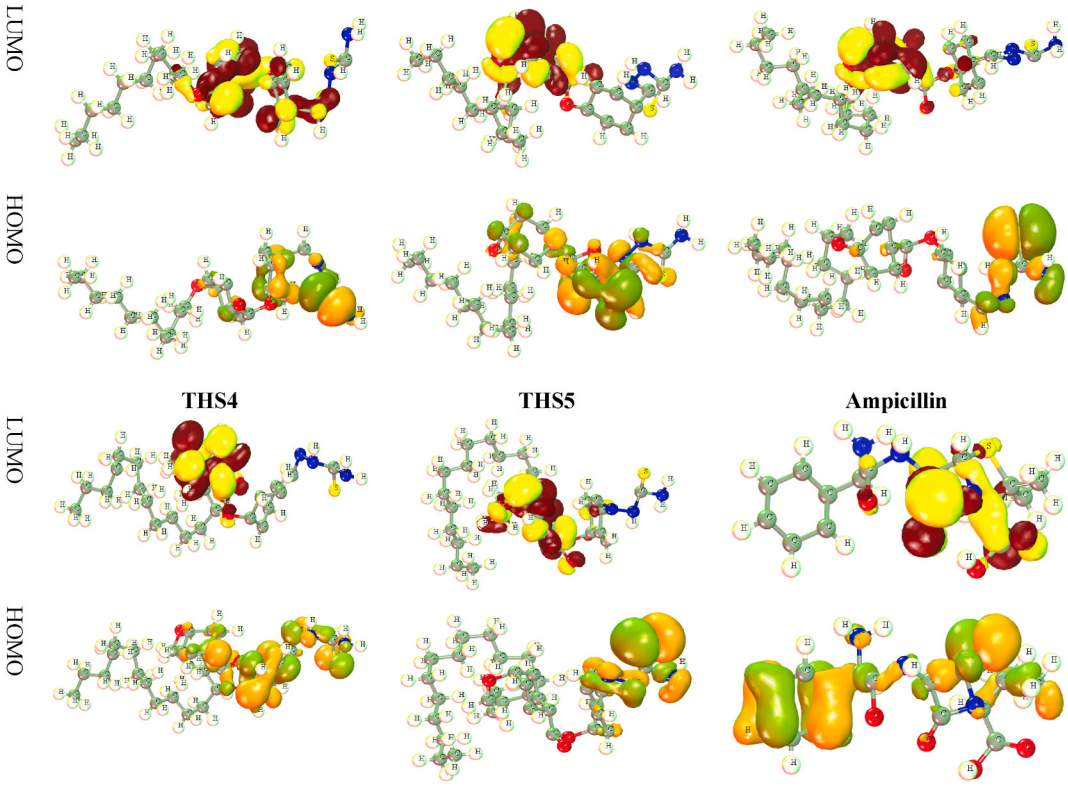

Fig. 3. Frontier molecular orbitals diagram for HOMO LUMO.

proliferates the interaction possibility of attachment mechanism of ligand and protein. From Fig. 4, it is found that the whole molecule is contained the negative and positive charge overall molecule having two parts. In the connection point, the charge is at 1.431, 2.28, −1.25, 2.47, 5.25, and 7.69. The red color contains the negative charge and the blue color is carried on the positive charge. In case of charge distribution, there are major part is blue inside of ring and molecule shown in Fig. 4. But the outer part has the red color where hydrogen atom is contained.

3.5. Pharmacokinetics and drug likeness study

Drug-likeness appraises the qualitatively a substance's potentiality of becoming an oral medication in term of bioavailability. Secondly, drug-like properties including the solubility, permeability, metabolic stability, transporter effects and bioavailability score, are vital factors to explain the structure of drug potential before synthesis. In addition, the Lipinski's five-rule is also related to the Drug-likeness. Lipinski's five-rule consists of the five parameters, such as 5 hydrogen bond donor, 10 hydrogen bond acceptor, total topological surface area, Log P (CLog P) does not excess than 5 and molecular weight is less than 500 g, if these are obey the mentioned condition, called small molecules for drugs. So, from Table S1, the bioavailability score is listed at 0.55 for THS1, THS2, Ampicillin, and staring, but it is abated for at 0.17 for THS3, THS4, and THS5. Secondly, utilizing of Lipinski's five-rule, the compounds of THS1, THS2, Ampicillin and staring are satisfied the Lipinski's five-rule, but THS3, THS4, and THS5 are opposite to Lipinski five-rule, because it can violate the one rule of molecular weight having large mass. Next, the low GI absorption index is obtained for all molecules whereas the starting conveys the high GI absorption index.

3.6. ADME studies

ADME properties are one of the foremost things becoming the bioactive molecule through the absorption, distribution, metabolism, and excretion (ADME). Having the numerous descriptors for ADME, there is involved the nine parameters, such as human intestinal absorption (HIA), blood-brain barrier (BBB), Caco-2 permeability, human intestinal absorption, P–I glycoprotein inhibitor, P-II glycoprotein substrate, renal organic cation, sub-cellular localization, CYP4502C9 substrate, and CYP4501A2 inhibitor shown in Table S2.

BBB conducts the protection of brain infections by the toxin or pathogens, as well as it allows the vital nutrient products to reach in brain. From the data, they are shown the positive magnitude, means that they can carry on the nutrient for brain system.

HIA submits for any drug that it is orally administrated by absorption from gastrointestinal system into the bloodstream of the human body. Our synthetic drugs are highly response to HIA; stands for high possibility of absorption by bloodstream from gastrointestinal system. In general, it is common fact that P-glycoprotein can protect the body system from the harmful materials. However, if P-glycoprotein is inhibited by any drug, the protection of body system will be hampering or harmful chemical will be stored in kidney, liver, lumen or other organs. However, the studied compounds can show the negative value in terms of P–I glycoprotein inhibitor, P-II glycoprotein substrate, CYP4502C9 substrate and CYP4501A2 inhibitor; means that there are no scope of harmful effect by them in body organs. Consequently, the Lysosome is the subcellular localization or Ampicillin, although all molecules and starting are in Mitochondria.

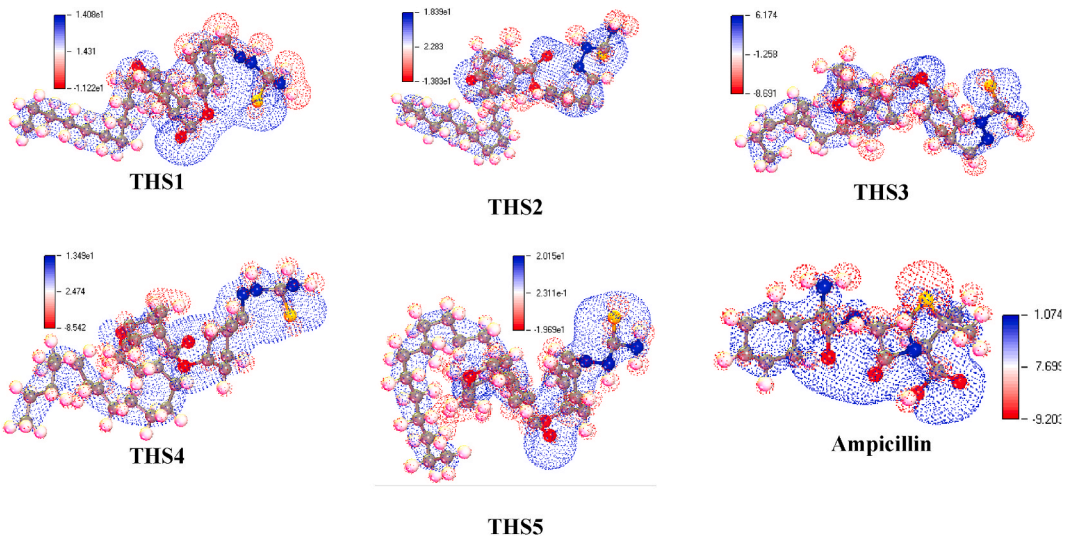

Fig. 4. Electrostatic potential charge distribution map.

3.7. Toxicity

The aquatic and non-aquatic environment is the most important fact for chemical species after use. The pragmatic fact of the toxicity is included to the water solubility (Log S), and the higher solubility mentions the higher toxicity of these molecules. In addition, the AMES toxicity, carcinogenicity, plasma protein binding, acute oral toxicity, oral rat acute toxicity, fish toxicity,T. Pyriformis toxicity were calculated for evaluating for the toxicity data listed in Table S3. First of all, the thiosemicarbazones and their derivatives convey the negative outcome for AMES toxicity and carcinogenicity. But the water solubility is at −4.455 for all derivates which is higher than starting even standard. The similar trend is found for plasma protein binding, acute oral toxicity, oral rat acute toxicity, fish toxicity, T. Pyriformistoxicity.

3.8. Calculation of QSAR and pIC_{50}

Quantitative structure activities relationship (QSAR) calculation has been performed to determine the relationship between biological activities and structural activities of chemical compounds using the computational method**.** The overall value of QSAR and pIC_{50} investigation meets all the criteria and it is observed that different compounds have different QSAR and pIC_{50} shown in Table S4. For calculation of $pIC_{50,}$ here most acceptable descriptors, such as Chiv5, bcutm1, MRVSA9, MRVSA6, PEOEVSA5, GATSv4, J and Diametert, were used for selected the thiosemicarbazones and their derivatives. It is found the range of QSAR and pIC_{50} between 4.094 and 6.492. It is noted for the thiosemicarbazones and their derivatives that with increasing the molecular mass or alkyl chain, the pIC_{50} has increased but is lower than 10.0. The estimated pIC_{50} suggests that these reported compounds might be biologically useful against bioactive molecules.

3.9. Molecular docking

Molecular docking assays were done in order for bioactive chemical species and proteins to be able to attach together and confirm the evidence for drug compound binding affinity [41]. An important part of molecular drug design focuses on the protein-ligand interaction. The hydrogen bonds, hydrophobic bonds, van der Waal bonds, and halogen bonds are the most significant considerations for binding the active site of protein to produce docking score as binding affinity where the docking score over 6.00 kcal/mol has been accepted as standard drug [42–45].

3.9.1. Molecular docking against bacteria

Table 2 conveys the binding affinity of thiosemicarbazones and their derivatives against seven human pathogenic bacteria, such as Histoplasma-capsulatum, E-coli, Salmonella-typhi, Shigella-flexneria, Staphylococcus-aureus, Staphylococcus-hominis, and Cryptococcus-neoforman. The binding affinity against Histoplasma-capsulatum, E-coli for all of thiosemicarbazones and its derivatives is recorded in above −6.0 kcal/mol, which is almost very close to standard even so much higher from starting. Among all bacteria, the highest binding affinity obtained against Salmonella-typhi stain, at which the THS2 conveys the excellent binding affinity (−8.80 kcal/mol) that is higher than the standard, Ampicillin (−8.60 kcal/mol), and THS3 and THS4 illustrate slightly lower binding affinity (−8.4 kcal/mol) having 2nd position among all derivatives.

3.9.2. Molecular docking against black fungus

For the antifungal activity of thiosemicarbazones and their derivatives, the most common fungal stains (Rhizomucor mieh, Mucor lusitanicus, Mycolicibacterium smegmatis and Aspergillus niger) have been chosen for molecular docking study. To say more, the black fungus infection-commonly known as the mucormycosis which is caused by Rhizomucor mieh, Mucor lusitanicus, and Mycolicibacterium smegmatis fungi as a result, this study conveys the binding activity of thiosemicarbazones and its derivatives against the black fungus strains. Table 3 shows the binding affinity of black fungus strain and *Aspergillus niger* strain while it is obtained that the binding affinity against *Rhizomucor mieh* is the highest among other stains, and THS3 conveys the higher binding affinity (−7.7 kcal/mol) than standard, Ampicillin (−7.6 kcal/mol) against *Rhizomucor mieh* even other stains.

3.9.3. Molecular docking against white fungus

Table 4 represents the binding affinity against Candida Auris, Aspergillus luchuensis, and Candida albicans fungal strains which are

Table 2
Binding affinity against bacteria.

Ligand No	*Histoplasma capsulatum (2jv7)*	*E.coli (6ch3)*	*Salmonella typhi (1wvg)*	*Shigellaflexneria (1z67)*	*Staphylococcus-aureus (3ip4)*	*Staphylococcus hominis(6exs)*	*Cryptococcus neoformans (5xu6)*
THS1	−6.0	−6.3	−8.1	−6.3	−5.6	−7.6	−6.0
THS2	−6.6	−7.0	−8.8	−5.8	−6.0	−6.7	−7.2
THS3	−6.5	−6.6	−8.4	−5.5	−5.9	−6.4	−6.3
THS4	−6.2	−6.5	−8.4	−5.5	−6.3	−6.5	−6.7
THS5	−6.6	−6.4	−8.0	−5.5	−5.5	−7.7	−6.0
Ampicillin	−6.7	−7.3	−8.7	−7.2	−6.7	−7.8	−7.3
Starting	−5.0	−5.1	−6.0	−5.2	−5.7	−6.1	−6.3

Table 3
Binding affinity against black fungus.

Ligand No	*Rhizomucor mieh(4WTP)*	*Mucor lusitanicus (6ZDW)*	*Mycolicibacterium smegmatis (7D6X)*	*Aspergillus niger (1kul)*
THS1	−7.0	−6.2	−7.4	−5.4
THS2	−7.7	−5.4	−7.1	−4.6
THS3	−7.5	−5.5	−7.6	−4.6
THS4	−7.4	−6.0	−6.7	−5.1
THS5	−6.5	−5.9	−7.4	−4.8
Ampicillin	−7.6	−6.2	−6.9	−5.9
Starting	−5.7	−4.6	−6.5	−5.1

Table 4
Binding affinity against white fungus strain.

Ligand No	*Candida Auris (6U8J)*	*Aspergillus luchuensis(1BK1)*	*Candida albicans (5HW7)*
THS1	−7.0	−8.1	−5.7
THS2	−6.7	−8.0	−6.5
THS3	−6.2	−7.6	−6.2
THS4	−6.0	−7.2	−6.1
THS5	−5.9	−7.0	−6.0
Ampicillin	−6.7	−8.7	−6.6
Starting	−5.9	−6.1	−4.9

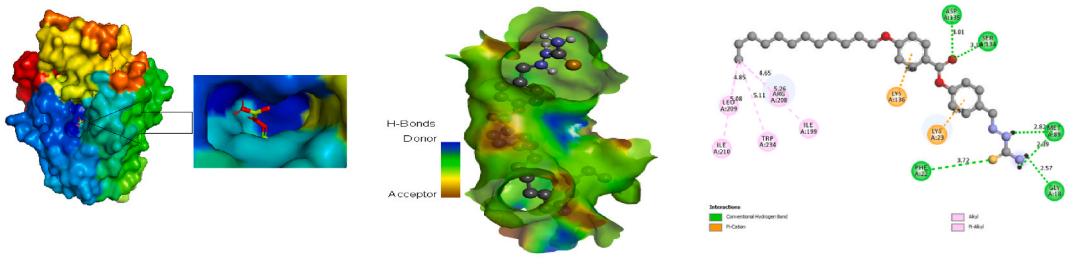

Docking pose of THS2 against Salmonella-typhi (1wvg)

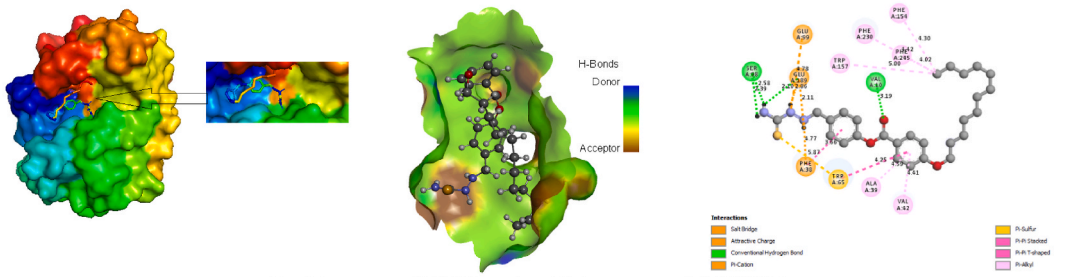

Docking pose of THS2 against Rhizomucor mieh(4WTP)

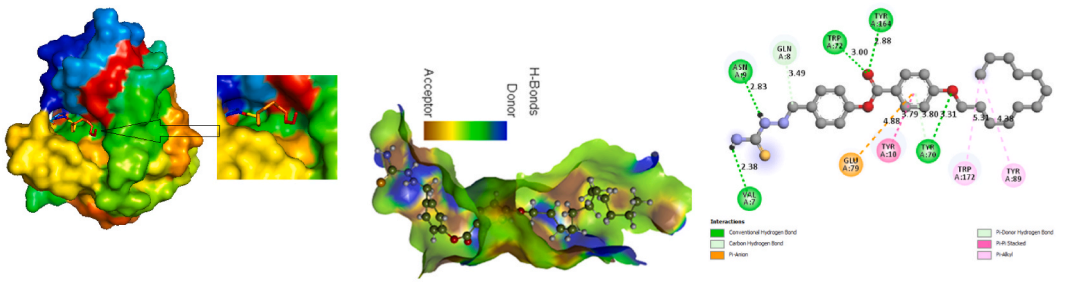

Docking pose of THS2 against Aspergillus luchuensis(1BK1)

Fig. 5. Docking poses for THS2 against various pathogens.

caused for the white fungus infection. From Table 4 and it is revealed that thiosemicarbazones and its derivatives show effective binding affinity against white fungal stains. Here, the binding energy of THS1 and THS2 is at −8.1 and −8.0 kcal/mol respectively while its value for Ampicillin is slightly higher (−8.7 kcal/mol) against *Aspergillus luchuensis* (1BK1). So, it can be said that the derivatives are potential against white fungus.

3.10. Protein-ligand interaction and active sites

The Discovery Studio software program can give the access to determine the protein to ligand interaction view and where the ligand is bonded with protein. Secondly, the number of hydrogen bond is one of the pivotal factors for determination of the blocking of active sites of protein by drug, and it is contributed to make a large binding energy. Moreover, hydrophobic nature can help to produce the linkages between non-polar endpoints, such as the benzene ring, heterocyclic ring and alkyl chain with protein or active sites shown in Fig. 5 with various docking poses. Moreover, the ligand protein interaction and bond distance are listed in Table S5, Table S6 and Table S7. From the interaction, it can be found that each of ligand can produce the conventional hydrogen bond that must indicate the higher potential as drug.

3.11. Molecular dynamics

There are several aspects in the molecular dynamics that evaluate the stability of molecule interaction. Besides that, MD is one of the major tools to ascertain molecular interaction and its stability. This has been calculated the RMSD and RMSF principles in the protein-ligand complex after simulating the molecular dynamics. With any statistic, the widely valid range of these two parameters has been declared below 2.0 Å (61, 62).

From Fig. 6, Fig. 6(a) and (b), the RMSD value of this studies ILs has been ascertained below 0.8 Å versus time. Besides, the RMSD range has also been ascertained below 0.8 against amino acid residues. Secondly, the RMSF value Fig. 6(c), Protein backbone interface with amino acid residue engagement was kept beneath 0.7 Å in terms of duration and amino acid framework.

In the case of the black fungus strain, the MD was performed against the Rhizomucor mieh strain for THS2, THS3, THS4 and standard. The foremost brief of MD from Fig. S2 is written as that all of the ligand proteins complexes for THS2, THS3, THS4 and standard are highly stable while the standard and THS3 are slightly higher stable than the other two. At last for the view of Aspergillus luchuensis as a white fungus strain, the similar ligands, THS2, THS3, THS4 and standard, have been taken for evaluation for the MD listed in Fig. S3. From Fig. S3(a), it is observed that the RMSD is slightly variable from each other although stays in the stable configuration which trend is almost similar for RMSD: Amino acid vs. backbone and Amino acid vs. backbone.

3.12. Antibacterial studies

Table S8 represents the zone of inhibition against Staphylococcus aurious, Staphylococcus hominis, *Salmonella typhi* and Shigella flexneria bacteria. The control was used as the solvent, DCM, in which all of THS was dissolved for making the solution, and it shows zero activity in the same concentration. From the table of S8, it is shown that the thiosemicarbazones and their derivatives are potential drugs against Staphylococcus hominis and *Salmonella typhi* rather than other bacteria. In addition, THS4 conveys the high antibacterial activity at 10.0 mm against Staphylococcus aurious where the Standard shows 12.4 mm. Secondly, the THS2 and THS5 illustrate the potential activity against Staphylococcus hominis.

In the case of antibacterial activity, the effect of the alkyl part in the thiosemicarbazones and their derivatives are estimated using the number of carbon in the alkyl chain. For each bacteria pathogen, the alkyl group has to be shown an effect on antibacterial activity. Moreover, it can be revealed that with increasing the alkyl chain, the zone of inhibition is slowly increased shown in Fig. 7(a) and the various zone of inhibition is added in Fig. 7(b).

4. Conclusion

The thiosemicarbazones and their derivatives were optimized using the DFT functional and obtained the structures. From the DFT

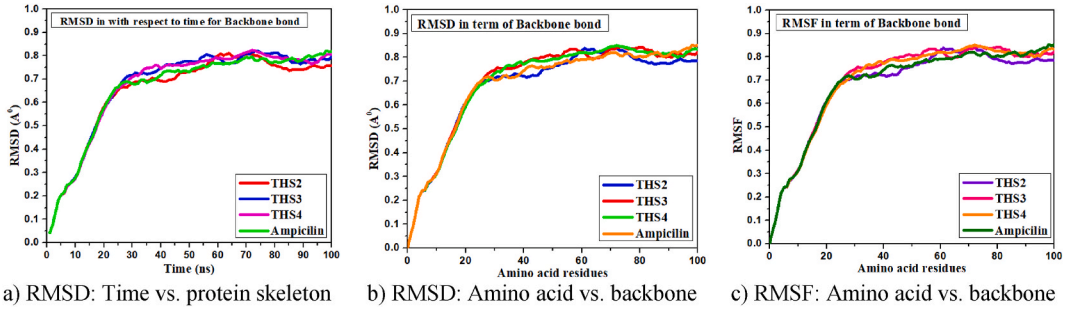

a) RMSD: Time vs. protein skeleton b) RMSD: Amino acid vs. backbone c) RMSF: Amino acid vs. backbone

Fig. 6. Various picture of RMSD and RMSF for *Salmonella-typhi* (1wvg).

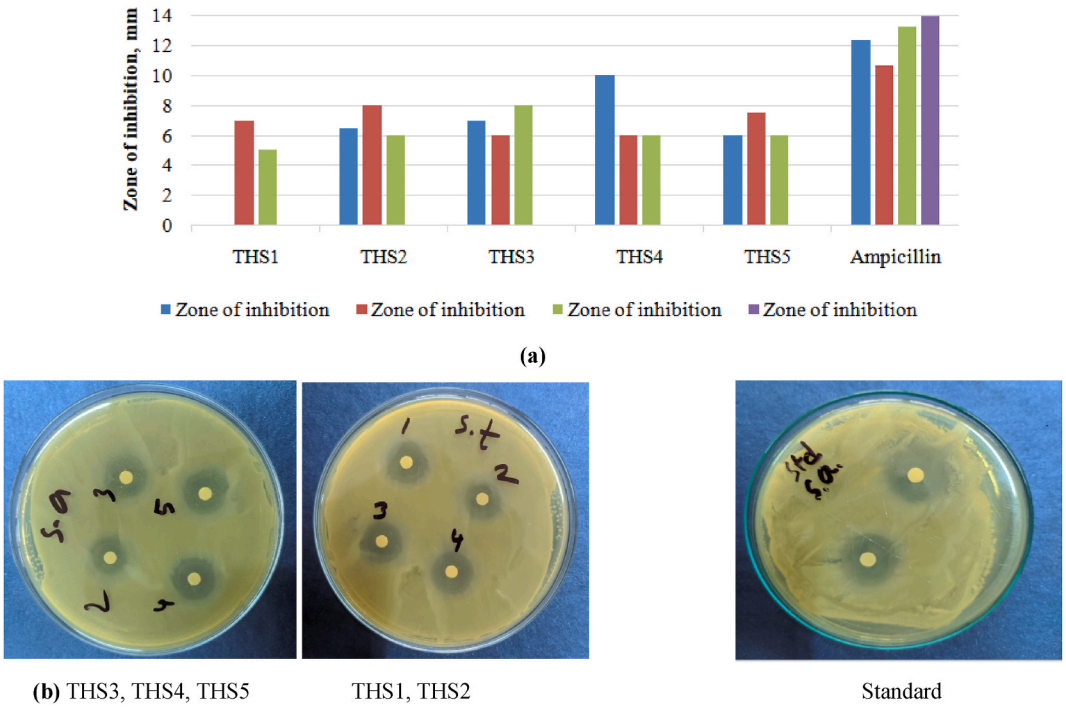

Fig. 7. (a) Effect of alkyl chain on antimicrobial activity, (b) picture of zone of inhibition for *Staphylococcus aurious*.

calculation, the HOMO, LUMO, and chemical descriptors were calculated at which the softness and hardness values are reasonable for becoming drugs. The energy gap obtained from HOMO and LUMO is varied to compounds, it is at 6.80 for standard and 4.458 for THS5 which is much lower than starting (7.535). It is revealed from the quantum calculation that the longest chain conveys the highest chemical reactivity as well as the biological significance. Next, the THS1, THS2, THS3 have satisfied the Lipinski rule for becoming small drug molecules although other (THS4, and THS5) have a high bioavailability score. Next, the ADMET shows that they illustrate low toxicity, non-carcinogenicity, and both aquatic and non-aquatic toxicity. With the appropriate fitting of ADMET, bioavailability score, and Lipinski rule, these were performed against seven human pathogenic bacteria, black fungus, and white fungus for primary screening their antimicrobial activity through the binding affinity using molecular docking tools. It is conveyed that the THS1, THS2, THS3, THS4, and THS5 are potential antimicrobial agents against these pathogens, and illustrated the highest activity in white fungus. In summarized by quantum calculation and molecular docking study, it is so sophisticated to make a co-relation between them. First of all, as there are attached five alkyl chains ($C_{10}H_{21}$, $C_{12}H_{25}$, $C_{14}H_{29}$, $C_{16}H_{33}$, and $C_{18}H_{37}$) is donated by THS1, THS2, THS3, THS4, and THS5, respectively where increasing the alkyl chain from THS1 to THS5, the energy gap is decreased regular fashion, as well as hardness and softness show the opposite trend. In addition, the binding affinity from molecular docking is slightly increased by soaring alkyl chain. After completing the computational investigation, these were synthesized through multi-step synthesis methods, such as alkylation, acidification, esterification, and formed the 4-(4′-alkoxybenzoyloxy) thiosemicarbazones. Then, the ^{1}H NMR, FTIR spectra, and melting point data give a good support to the conversion of reaction and their optimized chemical structure. In the end, the in-vitro test was done against Staphylococcus aurious, Staphylococcus hominis, *Salmonella typhi* and Shigella flexneria, and obtained a reasonable antibacterial activity compared to standard. From the in-vitro and *in-silico* study, all show the highest potential activity against *Salmonella typhi* although it is partially higher against white fungus on basis of *in-silico* study.

Author contribution statement

Mahbub Alam, Md. Mosharef Hossain Bhuiyan: Performed the experiments.
Mohammed Nurul Abser: Contributed reagents, materials, analysis tools or data.
Ajoy Kumer: Conceived and designed the experiments; Wrote the paper.
Parul Akter, Md. Emdad Hossain, Unesco Chakma: Analyzed and interpreted the data.

Data availability statement

No data was used for the research described in the article.

Additional information

No additional information is available for this paper.

Declaration of competing interest

The authors declare that they have no conflict of interest. All authors gave final approval for publication.

Acknowledgment

Authors are acknowledged to Department of Chemistry, Jahingirnagar University of Bangladesh, Savar, Dhaka −1342, Bangladesh for all kind of supports.

Appendix A. Supplementary data

Supplementary data to this article can be found online at https://doi.org/10.1016/j.heliyon.2023.e16222.

References

[1] T.S. Lobana, Bonding and structure trends of thiosemicarbazone derivatives of metals—an overview, Coord. Chem. Rev. 253 (2009) 977–1055.
[2] H. Khan, Synthesis, characterization and anticancer studies of mixed ligand dithiocarbamate palladium (II) complexes, Eur. J. Med. Chem. 46 (2011) 4071–4077.
[3] H. Beraldo, D. Gambino, The wide pharmacological versatility of semicarbazones, thiosemicarba-zones and their metal complexes, Mini Rev. Med. Chem. 4 (2004) 31–39.
[4] P. Chellan, et al., Exploring the versatility of cycloplatinated thiosemicarbazones as antitumor and antiparasitic agents, Organometallics 31 (2012) 5791–5799.
[5] B. Demoro, et al., New organoruthenium complexes with bioactive thiosemicarbazones as co-ligands: potential anti-trypanosomal agents, Dalton Trans. 41 (2012) 1534–1543.
[6] F. Vandresen, et al., Novel R-(+)-limonene-based thiosemicarbazones and their antitumor activity against human tumor cell lines, Eur. J. Med. Chem. 79 (2014) 110–116.
[7] G.L. Parrilha, et al., Applications of radiocomplexes with thiosemicarbazones and bis (thiosemicarbazones) in diagnostic and therapeutic nuclear medicine, Coord. Chem. Rev. 458 (2022), 214418.
[8] W.-x. Hu, et al., Synthesis and anticancer activity of thiosemicarbazones, Bioorg. Med. Chem. Lett 16 (2006) 2213–2218.
[9] C. Lambros, et al., In vitro assessment of 2-acetylpyridine thiosemicarbazones against chloroquine-resistant Plasmodium falciparum, Antimicrob. Agents Chemother. 22 (1982) 981–984.
[10] H.P. Ebrahimi, et al., A novel series of thiosemicarbazone drugs: from synthesis to structure, Spectrochim. Acta Mol. Biomol. Spectrosc. 137 (2015) 1067–1077.
[11] Y. Zhou, V.M. Lauschke, Computational tools to assess the functional consequences of rare and noncoding pharmacogenetic variability, Clin. Pharmacol. Ther. 110 (2021) 626–636.
[12] M. Korshunova, et al., OpenChem: a deep learning toolkit for computational chemistry and drug design, J. Chem. Inf. Model. 61 (2021) 7–13.
[13] H.E. Hashem, A. Nath, A. Kumer, Synthesis, molecular docking, molecular dynamic, quantum calculation, and antibacterial activity of new Schiff base-metal complexes, J. Mol. Struct. 1250 (2022), 131915, https://doi.org/10.1016/j.molstruc.2021.131915.
[14] D. Howlader, M.S. Hossain, U. Chakma, A. Kumer, M.J. Islam, M.T. Islam, T. Hossain, J. Islam, Structural geometry, electronic structure, thermo-electronic and optical properties of $GaCuO_2$ and $GaCu_{0.94}Fe_{0.06}O_2$: a first principle approach of three DFT functionals, Mol. Simulat. 47 (2021) 1411–1422, https://doi.org/10.1080/08927022.2021.1977295.
[15] M.E. Kobir, A. Ahmed, Roni MAH, U. Chakma, M.R. Amin, A. Chandro, A. Kumer, Anti-lung cancer drug discovery approaches by polysaccharides: an in silico study, quantum calculation and molecular dynamics study, J. Biomol. Struct. Dyn. (2022) 1–17, https://doi.org/10.1080/07391102.2022.2110156.
[16] M.N. Sarker, A. Kumer, M.J. Islam, S. Paul, A computational study of thermophysical, HOMO, LUMO, vibrational spectrum and UV-visible spectrum of cannabicyclol (CBL), and cannabigerol (CBG) using DFT, Asian J. Nanosci. Mater. 2 (2019) 439–447, https://doi.org/10.26655/AJNANOMAT.2019.4.8.
[17] A. Zannat, A. Kumar, M.N. Sarker, S. Paul, The substituent group Activity in the anion of cholinium carboxylate ionic liquids on thermo-physical, chemical reactivity, and biological properties: a DFT study, Int. J. Chem. Technol. 3 (2019) 151–161, https://doi.org/10.32571/ijct.648409.
[18] M.M. Hoque, A. Kumer, M.S. Hussen, M.W. Khan, Theoretical evaluation of 5, 6-diaroylisoindoline-1, 3-dione as potential carcinogenic kinase PAK1 inhibitor: DFT calculation, molecular docking study and ADMET prediction, Int. J. Adv. Biol. Biomed. Res. 9 (2021) 77–104, https://doi.org/10.22034/ijabbr.2021.45696.
[19] M.I. Hossain, A. Kumer, Synthesis and characterization of ammonium benzoate and its derivative based ionic liquids and their antimicrobial studies, Asian J. Phys. Chem. Sci. 5 (2018) 1–9, https://doi.org/10.9734/AJOPACS/2018/39148.
[20] M.J. Islam, M.N. Sarker, A. Kumer, S. Paul, The evaluation and comparison of thermo-physical, chemical and biological properties of palladium (II) complexes on binuclear amine ligands with different anions by DFT study, Int. J. Adv. Biol. Biomed. Res. 7 (2019) 315–334, https://doi.org/10.33945/SAMI/IJABBR.2019.4.3.
[21] A. Kumer, U. Chakma, Mohammed M. Matin, S. Akash, A. Chandro, D. Howlader, The computational screening of inhibitor for black fungus and white fungus by D-glucofuranose derivatives using in silico and SAR study, Org. Commun. 14 (2021), https://doi.org/10.25135/acg.oc.116.2108.2188.
[22] A. Kumer, M.W. Khan, Synthesis, characterization, antimicrobial activity and computational exploration of ortho toludinium carboxylate ionic liquids, J. Mol. Struct. 1245 (2021), 131087.
[23] M.A. Rahman, M.M. Matin, A. Kumer, U. Chakma, M. Rahman, Modified D-glucofuranoses as new black fungus protease inhibitors: computational screening, docking, dynamics, and QSAR study, Phys. Chem. Res. 10 (2022) 195–209, https://doi.org/10.22036/pcr.2021.294078.1934.
[24] B. Delley, DMol, a standard tool for density functional calculations: review and advances, Theor. Comput. Chem. 2 (1995) 221–254.
[25] A. Daina, et al., SwissADME: a free web tool to evaluate pharmacokinetics, drug-likeness and medicinal chemistry friendliness of small molecules, Sci. Rep. 7 (2017) 1–13.
[26] F.L. Cheng, Weihua, Yadi Zhou, Jie Shen, Zengrui Wu, Guixia Liu, Philip W. Lee, Yun Tang, admetSAR: a comprehensive source and free tool for assessment of chemical ADMET properties, J. Chem. Inf. Model. 52 (2012) 3099–3105, https://doi.org/10.1021/ci300367a.
[27] C.L. Hongbin Yang, Lixia Sun, Jie Li, Yingchun Cai, Zhuang Wang, Weihua Li, Guixia Liu, Yun Tang, admetSAR 2.0: web-service for prediction and optimization of chemical ADMET properties, Bioinformatics 35 (2018) 1067–1069, https://doi.org/10.1093/bioinformatics/bty707.

[28] H.L. Yang, Chaofeng, Lixia Sun, Jie Li, Yingchun Cai, Zhuang Wang, Weihua Li, Guixia Liu, Yun Tang, admetSAR 2.0: web-service for prediction and optimization of chemical ADMET properties, Bioinformatics 35 (2019) 1067–1069.
[29] W.L. DeLano, The PyMOL user's manual. http://www.pymol.org, 2002.
[30] S. Dallakyan, A.J. Olson, Small-molecule Library Screening by Docking with PyRx, Chemical biology: methods and protocols, 2015, pp. 243–250.
[31] A. S. Inc. Discovery Studio Modeling Environment, Release 4.0 [Online].
[32] A. Kumer, U. Chakma, M.M. Matin, Bilastine based drugs as SARS-CoV-2 protease inhibitors: molecular docking, dynamics, and ADMET related studies, Orbital - Electron. J. Chem. 14 (2022) 15–23, https://doi.org/10.17807/orbital.v14i1.1642.
[33] M. Rani, A. Nath, A. Kumer A, In-silico investigations on the anticancer activity of selected 2-aryloxazoline derivatives against breast cancer, J. Biomol. Struct. Dyn. (2022) 1–10, https://doi.org/10.1080/07391102.2022.2134208.
[34] A. Kumer, M.N. Sarker, S. Paul, The theoretical investigation of HOMO, LUMO, thermophysical properties and QSAR study of some aromatic carboxylic acids using HyperChem programming, Int. J. Chem. Technol. 3 (2019) 26–37, https://doi.org/10.32571/ijct.478179.
[35] A. Kumer, M.N. Sarker, S. Paul, The thermo physical, HOMO, LUMO, Vibrational spectroscopy and QSAR study of morphonium formate and acetate Ionic Liquid Salts using computational method, Turk. Comput. Theor. Chem. 3 (2019) 59–68, https://doi.org/10.33435/tcandtc.481878.
[36] A. Kumer, N.M. Sarker, S. Paul, A. Zannat, The theoretical prediction of thermophysical properties, HOMO, LUMO, QSAR and biological indics of cannabinoids (CBD) and tetrahhdrocannabinol (THC) by computational chemistry, Adv. J. Chem.-A 2 (2019) 190–202, https://doi.org/10.33945/SAMI/AJCA.2019.2.190202.
[37] R. Bonaccorsi, et al., Molecular SCF calculations for the ground state of some three-membered ring molecules:(CH2) 3,(CH2) 2NH,(CH2) 2NH2+,(CH2) 2O, (CH2) 2S,(CH) 2CH2, and N2CH2, J. Chem. Phys. 52 (1970) 5270–5284.
[38] E. Scrocco, J. Tomasi, The electrostatic molecular potential as a tool for the interpretation of molecular properties, in: New Concepts II, Springer, 1973, pp. 95–170.
[39] P. Politzer, D.G. Truhlar, Chemical Applications of Atomic and Molecular Electrostatic Potentials: Reactivity, Structure, Scattering, and Energetics of Organic, Inorganic, and Biological Systems, Springer Science & Business Media, 2013.
[40] J.J. Müller, et al., Modeling of electrostatic recognition processes in the mammalian mitochondrial steroid hydroxylase system, Biophys. Chem. 100 (2002) 281–292.
[41] A.K.S. Babahedari, E. Heidari, M Karimi Shamsabadi, H. Kabiri, The comprehensive evaluation docking of methicillin drug containing isoxazole derivatives, as targeted antibiotics to Staphylococcus aureus, J. Bionanosci. 7 (2013) 288–291, https://doi.org/10.1166/jbns.2013.1119.
[42] A. Kumer, M.W. Khan, Synthesis, characterization, antimicrobial activity and computational exploirations of ortho toludinium carboxylate ionic liquids, J. Mol. Struct. (2021), 131087, https://doi.org/10.1016/j.molstruc.2021.131087.
[43] A. Kumer, K. Md Wahab, The effect of alkyl chain and electronegative atoms in anion on biological activity of anilinium carboxylate bioactive ionic liquids and computational approaches by DFT functional and molecular docking, Heliyon 7 (2021), e07509, https://doi.org/10.1016/j.heliyon.2021.e07509.
[44] A. Nath, Ajoy Kumer, Md Wahab Khan, Synthesis, computational and molecular docking study of some 2, 3-dihydrobenzofuran and its derivatives, J. Mol. Struct. 1224 (2020) 129–225, https://doi.org/10.1016/j.molstruc.2020.129225.
[45] A. Nath, A. Kumer, K.F. Zaben, Md Wahab, Investigating the binding affinity, molecular dynamics, and ADMET properties of 2, 3-dihydrobenzofuran derivatives as an inhibitor of fungi, bacteria, and virus protein, Beni-Suef Univ. J. Basic Appl. Sci. vol. 10 (2021) 1–13, https://doi.org/10.1186/s43088-021-00117-8.